

## Original Article

## Optical coherence tomography angiography measured capillary density in normal and glaucoma eyes

## RPCs and ONH capillary density in glaucoma

Tarannum Mansoori<sup>a,\*</sup>; Jahnvi Gamalapati<sup>b</sup>; Jayanthi Sivaswamy<sup>b</sup>; Nagalla Balakrishna<sup>c</sup>

## Abstract

**Purpose:** To compare the diagnostic ability of optical coherence tomography angiography (OCT-A) derived radial peripapillary capillary (RPC) measured capillary density (CD) and inside the optic nerve head (ONH) CD measurements to differentiate between the normal and primary open angle glaucoma (POAG) eyes.

**Methods:** AngioVue disc OCT-A images were obtained and assessed in 83 eyes of POAG patients and 74 age matched healthy eyes. RPC CD was quantitatively measured in the peripapillary area within 3.45 mm circle diameter around the ONH and inside the ONH in 8 equally divided sectors, using Bar – Selective Combination of Shifted Filter Responses method after the suppressing large vessels. Area under receiver operating characteristic (AUROC) curve was used to assess the diagnostic accuracy of the two scanning regions of CD to differentiate between the normal and POAG eyes.

**Results:** The mean peripapillary RPC density ( $0.12 \pm 0.03$ ) and mean ONH CD ( $0.09 \pm 0.03$ ) were significantly lower in POAG eyes when compared to the normal eyes (RPC CD:  $0.17 \pm 0.05$ ,  $p < 0.0001$  and ONH CD  $0.11 \pm 0.02$ ,  $p = 0.01$  respectively). The POAG patients showed 29% reduction in the RPC CD and 19% reduction in the ONH CD when compared to the normal eyes. The AUROC for discriminating between healthy and glaucomatous eyes was 0.784 for mean RPC CD and 0.743 for the mean ONH CD.

**Conclusions:** Diagnostic ability of OCT-A derived peripapillary CD and ONH CD was moderate for differentiating between the normal and glaucomatous eyes. Diagnostic ability of even the best peripapillary average and inferotemporal sector for RPC CD and average and superonasal sector for the ONH CD was moderate.

**Keywords:** POAG, Peripapillary capillary density, OCT-A, ONH capillary density

© 2018 Production and hosting by Elsevier B.V. on behalf of Saudi Ophthalmological Society, King Saud University. This is an open access article under the CC BY-NC-ND license (<http://creativecommons.org/licenses/by-nc-nd/4.0/>). <https://doi.org/10.1016/j.sjopt.2018.09.006>

## Introduction

Glaucoma is a multi – factorial, progressive, optic neuropathy with complex pathophysiology, which is characterized by the retinal ganglion cell axonal degeneration. The role of optic nerve head (ONH) microvascular network in ocu-

lar blood flow and vascular dysfunction has been investigated in the pathogenesis of glaucoma.<sup>1</sup>

Radial peripapillary capillaries (RPC) are a unique plexus of capillary network, which display a characteristic linear morphological pattern with a minimal inter capillary anastomosis. They are restricted to the posterior pole and confined to the

Received 4 April 2017; received in revised form 30 August 2018; accepted 25 September 2018; available online xxxx.

<sup>a</sup> Anand Eye Institute, Hyderabad, India

<sup>b</sup> International Institute of Information Technology, Hyderabad, India

<sup>c</sup> National Institute of Nutrition, Hyderabad, India

\* Corresponding author at: Sita Lakshmi Glaucoma Center, Anand Eye Institute, 7-147/1, Nagendra Nagar, Habsiguda, Hyderabad 500007, India. e-mail address: [tarannummansoori@yahoo.com](mailto:tarannummansoori@yahoo.com) (T. Mansoori).



Peer review under responsibility of Saudi Ophthalmological Society, King Saud University



Production and hosting by Elsevier

Access this article online: [www.saudiophthaljournal.com](http://www.saudiophthaljournal.com) [www.sciencedirect.com](http://www.sciencedirect.com)

inner aspect of the retinal nerve fiber layer (RNFL) around the ONH.<sup>2</sup> Histological studies<sup>3,4</sup> and imaging studies with Optical coherence tomography angiography (OCT-A)<sup>5-11</sup> have highlighted the role of RPC and superficial retinal network in the pathogenesis of glaucoma.

OCT-A with split spectrum amplitude-decorrelation angiography (SSADA) algorithm is a new imaging modality that can be used to visualize retinal and ONH vasculature in the various retinal layers<sup>12</sup> and provides quantitative measurement of the microcirculation in the peripapillary region<sup>7,9,10</sup> and ONH<sup>6,10,11</sup> vessel density.

Bar – Selective Combination of Shifted Filter Responses (B-COSFIRE) filter method is very effective in the detection and quantitative estimation of the capillaries.<sup>13</sup> A study by our group has evaluated topological and quantitative measurement of the OCT-A derived RPC network in the normal healthy eyes with good intra-visit intra-operator repeatability using B-COSFIRE method.<sup>14</sup>

The purpose of the current study was to compare the diagnostic ability of OCT-A derived peripapillary RPC capillary density (CD) and inside ONH CD for differentiating healthy eyes and primary open angle glaucoma (POAG) eyes.

## Material and methods

For this prospective study, healthy subjects and POAG patients were enrolled after obtaining the informed consent. The study was performed in accord with the tenets of the Declaration of Helsinki for the research involving human subjects.

All the participants underwent comprehensive ophthalmic examination, including medical history, assessment of best-corrected visual acuity, slit-lamp biomicroscopy examination, intraocular pressure (IOP) measurement with Goldmann applanation tonometry, gonioscopy with Sussman gonioscopes, central corneal thickness (CCT) pachymetry measurement with AL scan (Nidek CO, Ltd, Gamagori, Japan), dilated fundus examination and perimetry with Swedish interactive thresholding algorithm (SITA) standard 24-2 program using Humphrey field analyzer (HFA 720 II Carl Zeiss Meditec, Dublin, California, USA). OCT-A and spectral domain (SD) OCT images were obtained by two experienced operators on the same visit using the dual modality RTVue XR-100 OCT (Avanti, Optovue Inc., Fremont, CA, version 2015.1.0.90).

Healthy subjects had no history of elevated IOP, no family history of glaucoma, IOP < 21 mm Hg, normal anterior and posterior segment on clinical examination, normal optic disc with intact neuroretinal rim and RNFL, reliable and normal visual fields (defined as a Pattern standard deviation (PSD) within 95% confidence limits and Glaucoma Hemifield Test result within normal limits). Visual fields were considered reliable if the fixation losses were ≤20% and false-negative errors and false-positive errors were ≤15%, with no lens rim or eyelid artifacts.

POAG patients had IOP > 21 mmHg, open angles on gonioscopy, glaucomatous optic disc changes (Neuroretinal rim thinning, rim notching or RNFL defect) reliable and repeatable glaucomatous visual field defect defined as GHT outside normal limits and PSD outside 95% normal confidence limits.

Participants with a history of ocular trauma, intraocular surgery, co existing corneal or retinal pathology, neurological disease, non glaucomatous optic neuropathy, refractive error ≥ ±6 Diopter (D) sphere and cylinder ≥ ±3D, media opacities, unreliable visual field, poor quality OCT-A or ONH SD-OCT images, were excluded from the study.

## Optical coherence tomography angiography

### Image acquisition and processing

The AngioVue Avanti OCT is a noninvasive OCT-based method for visualizing the ONH and retinal vasculature. It uses a 840-nm wavelength light source and a bandwidth of 50 nm. It has an A-scan rate of 70,000 scans per seconds, axial resolution of 5 μm in tissue and a 22 μm focal spot diameter. Each volume contains 304 × 304 A-scans with two consecutive B-scans captured at a each fixed position. Each image set comprises of a set of 2 scans: one vertical priority (y-fast) and one horizontal priority (x-fast) raster volumetric pattern. Each scan is acquired in less than 3 seconds. which minimizes the motion artifacts. An orthogonal registration algorithm is used to produce a 3 – dimensional OCT angiograms of the retinal vasculature by merging the 2 scans.<sup>15</sup> The SSADA method is used to compare the consecutive B scans at the same location to capture the dynamic motion of the red blood cells using motion contrast.<sup>12</sup> An enface angiogram of the RPC segment was obtained by the maximum flow (decorrelation value) projection which extends from the internal limiting membrane (ILM) to the posterior boundary of RNFL covering, 4.5 mm × 4.5 mm field of view and centered on ONH. An enface angiogram of the ONH segment was obtained in 4.5 × 4.5 mm field of view.

A trained examiner reviewed all the OCT-A scans and only the images with good clarity, a signal strength index (SSI) of more than 40, with no residual motion artifacts (irregular vessel pattern on the enface angiogram) were included for the analysis.

All the subjects also underwent ONH imaging with RTVue – XR-100 SD-OCT system with the ONH map protocol to obtain ONH structural measurements and peripapillary RNFL thickness measurements along a circle diameter of 3.45 mm centered on the ONH. The ONH scan is a combination of circular scans for RNFL thickness analysis and radial scans for ONH shape analysis, which ensures that the RNFL and ONH scan share the same center. Thirteen circle lines, with the diameters of 1.3–4.9 mm are scanned and used to create peripapillary RNFL map. The ONH scan consists of 12 radial lines of 3.7 mm length, 2.5–4 mm in diameter, which are used to calculate the disc margin and ONH parameters. Retinal pigment epithelium (RPE)/Bruch's membrane end tips are automatically detected on the radial image as the disc margin and disc area is calculated. Only good quality images, as defined by the scans with a SSI > 50, without segmentation or algorithm failure or artifacts were included.

The enface RPC angiogram images and the enface ONH angiogram image were transferred to a computer to quantify RPC CD and inside the ONH CD. The peripapillary and ONH region were equally divided into 8 equal sectors, which were designated as Superior nasal (SN), Superior temporal (ST), Temporal upper (TU), Temporal lower (TL), Nasal upper (NU), Nasal lower (NL), Inferior nasal (IN) and Inferior temporal (IT) (Fig. 1A and B). MATLAB (Mathworks version R 2014 a)

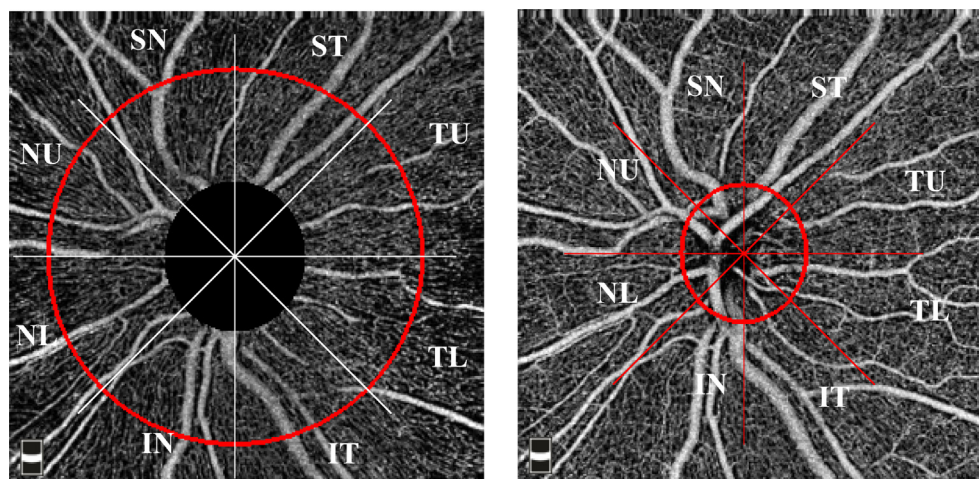


**Fig. 1.** A. Enface optical coherence tomography angiography image of the left eye of a normal subject: Radial peripapillary capillaries (RPC) and sectors where the RPC capillary density was calculated: Superior nasal (SN), Superior temporal (ST), Temporal upper (TU), Temporal lower (TL), Nasal upper (NU), Nasal lower (NL), Inferior nasal (IN) and Inferior temporal (IT). B. Enface optical coherence tomography angiography image of the optic nerve head (ONH) of the left eye in a normal subject and the sectors where the capillary density was calculated. Disc margin is marked by red elliptical outline.

software was used for the calculation of CD by a single trained examiner who was masked to the clinical findings.

For the RPCs CD analysis, the outer circle was chosen to be at 3.45 mm circle diameter around ONH for all the images, while inner circle is chosen as per the disc size for each eye and for the ONH CD analysis, a set of user-defined points on the ONH boundary was chosen and the best fit circle to these points was marked (Fig. 1B). Capillaries were detected using B-COSFIRE method for the automatic segmentation of blood vessels.<sup>13</sup> The method uses a difference of Gaussians (Do G) filter for vessel detection and the choice of parameters of the Gaussian determines the thickness of extracted vessels. These parameters were tuned to extract and suppress the large vessels. The Do G response is thresholded with a value 30 to obtain a binary mask where all the thick vessels are set to 0 and the others are set to 1. Multiplying this mask with the RPCs and ONH Angio flow image yields the desired capillary image ( $I_C$ ) with only the capillary network. The CD was calculated as:  $CD(i) = \frac{N_w(i)}{A(i)}$  where  $i = 1, 2 \dots 8$ , is the sector index,  $N_w(i)$  denotes the number of white pixels and  $A(i)$  denotes the area of the  $i$ th sector of  $I_C$ .

### Statistical analysis

Prior to comparison between the groups, numerical data was tested for assumption of homogeneity of variances using the Levene's test. Descriptive analysis were calculated as the mean and standard deviation. Unpaired  $t$  test was used to compare clinical parameters, CD and RNFLT parameters between the sectors in normal subjects and POAG eyes. Categorical variables were compared using the chi square test. Correlation of mean ONH CD with disc area was measured using Pearson's correlation coefficient. Area under the receiver operating characteristic (AUROC) curves were used to describe the diagnostic accuracy of RPC and ONH CD for differentiating between the healthy and POAG eyes. Statistical analysis was performed using commercial SPSS software (version 19, IBM, Chicago, USA). A  $P$  value  $< 0.05$  was considered statistically significant.

### Results

Seventy four eyes of 74 healthy subjects (mean age,  $53.1 \pm 14.1$  years) and 83 eyes of POAG patients (mean age,  $53.9 \pm 10.7$  years) were included in the study. In POAG group, 27 eyes had mild stage, 12 moderate stage and 37 had severe stage glaucoma, according to Hodapp-Parrish-Anderson grading scale of severity of visual field defect.<sup>16</sup> Of the 83 POAG eyes, 49 eyes were on prostaglandin analogues, 20 on combination of topical carbonic anhydrase inhibitor and beta blocker, and 14 on the alpha agonist. Self-reported history of hypertension and diabetes mellitus was more frequent in glaucoma patients when compared with the healthy controls but the difference was not significant (Table 1).

Statistically significant differences were found between glaucoma patients and healthy subjects for all ocular parameters except for IOP [POAG patients had IOP control with Anti-glaucoma medication (AGM)], CCT and the disc area. SSI of the OCT-A and ONH scan was significantly better in the normal eyes when compared to the POAG patients (Table 1).

### Qualitative assessment of the RPC and ONH CD

Healthy subjects had a dense peripapillary RPC network around the ONH and a dense microvascular capillary network inside the ONH, when compared to the eyes with POAG (Fig. 2A–C). There was focal capillary dropout of the RPC and ONH microvascular network in early (Fig. 2D and E) and moderate stage (Fig. 2F and G) glaucoma. In advanced stage of glaucoma the capillary network became sparser and more attenuated in the peripapillary and ONH region with diffuse capillary loss (Fig. 2H and I).

### Quantitative assessment of the RPC and ONH CD

The mean ( $\pm$ Standard deviation) RPC density was significantly lower in the POAG eyes ( $0.12 \pm 0.03$ ) when compared to the normal eyes ( $0.17 \pm 0.05$ ) ( $p < 0.0001$ ). The mean

**Table 1.** Ocular and clinical parameters of the study population.

Variables	Normal	Glaucoma	P value
Age (years)	53.13 ± 14.11	53.87 ± 10.73	<b>0.71</b>
Female/male	26/57	34/40	<b>0.06</b>
Self reported history of Diabetes mellitus	6	36	<b>0.05</b>
Self reported history of hypertension	14	30	<b>0.05</b>
Intraocular pressure (mm Hg)	14.27 ± 2.34	14.98 ± 3.13	<b>0.11</b>
Central corneal thickness (microns)	512.2 ± 27.9	513 ± 32.75	<b>0.87</b>
Mean deviation (Decibels)	-1.50 ± 0.74	-12.04 ± 8.51	<0.0001
Pattern standard deviation (Decibels)	1.67 ± 0.43	6.74 ± 5.16	<0.0001
Signal strength index (OCT-A)	71.73 ± 11.31	62.49 ± 9.02	<0.0001
Mean peripapillary capillary density	0.17 ± 0.05	0.12 ± 0.03	<0.0001
Mean inside Optic nerve head capillary density	0.11 ± 0.02	0.09 ± 0.03	0.01
Signal strength index (Optic nerve head)	70.38 ± 12.7	59 ± 9.77	<0.0001
Average Retinal nerve fiber layer (microns)	100.57 ± 10.31	75.46 ± 15.71	<0.0001
Cup disc vertical ratio	0.58 ± 0.14	0.85 ± 0.11	<0.0001
Cup disc horizontal ratio	0.67 ± 0.15	0.89 ± 0.11	<0.0001
Rim area (mm <sup>2</sup> )	1.25 ± 0.26	0.65 ± 0.26	<0.0001
Disc area (mm <sup>2</sup> )	2.23 ± 0.43	2.24 ± 0.5	<b>0.89</b>

OCT-A: Optical coherence tomography angiography.

inside ONH CD was significantly lower in POAG eyes ( $0.09 \pm 0.03$ ) when compared to the normal eyes ( $0.11 \pm 0.02$ ) ( $p = 0.01$ ) (Table 1).

There was no significant correlation between the disc area and mean ONH CD measurements in the healthy eyes (Pearson correlation coefficient =  $-0.18$ ,  $p = 0.115$ ) and POAG eyes (Pearson correlation coefficient =  $-0.15$ ,  $p = 0.154$ ) respectively.

Sector-wise analysis revealed that there was a significant difference between RPC CD and ONH CD measurements between the 2 groups, except for the CD of the superior temporal sector of the ONH ( $p = 0.09$ ) (Table 2).

The AUROC ± Standard error (SE) for discriminating between the healthy and glaucomatous eyes was  $0.784 \pm 0.038$  for mean RPC CD and  $0.743 \pm 0.052$  for the mean ONH CD (Table 3). The AUROC for the best parameter for RPC was CD in the IT sector ( $0.782 \pm 0.038$ ) and mean CD ( $0.784 \pm 0.038$ ). The AUROC for the best parameter for inside ONH CD was  $0.724 \pm 0.051$  for the SN sector CD and mean ONH ( $0.743 \pm 0.052$ ).

When 0.16 was taken as a cut off value for Mean RPC CD, the sensitivity was 88% and the specificity was 66.2% and for a cutoff value of 0.136 for the mean ONH CD, the sensitivity was 87.8% and the specificity was 58% for glaucoma detection.

## Discussion

In the present study, using OCT-A, the diagnostic accuracy of the two scanning areas i.e., RPC and ONH CD measurements were evaluated for differentiating POAG eyes from the normal eyes. OCT-A measured RPC CD and ONH CD showed focal or diffuse loss of CD based on the glaucoma severity.

In 12 normal and 12 glaucomatous eyes (Mean MD:  $-6.05 \pm 7.07$  dB), Liu et al.<sup>8</sup> reported AUROC of 0.94 and specificity of 91.7% and sensitivity of 83.3% for peripapillary vessel density measures in a thicker slab from ILM to RPE. Another study evaluated the microvascular bed in the RNFL layer, (which largely reflects the RPCs), and found that the OCT-A circumpapillary vessel density measurement had AUROC of 0.83 for glaucoma detection in 23 healthy and

104 glaucoma subjects (Median MD:  $-3.9$  dB).<sup>5</sup> Rao et al.<sup>9</sup> reported that the AUROCs of the average peripapillary vessel density was 0.83 for differentiating between the normal (78 eyes) and POAG patients (64 eyes, Median MD:  $-5.3$  dB). Mammo et al.<sup>7</sup> used a manual tracing technique to quantify RPCs density in the images of Speckle variance OCT-A and reported that the density of RPCs was significantly lower in glaucomatous eyes ( $n = 10$ ) when compared with matched - peripapillary regions in normal eyes ( $n = 16$ ). Wang et al.<sup>10</sup> reported an AUROC of 0.8 for the ONH vessel density, in 20 normal and 62 POAG patients.

We found that the AUROC of ONH CD was highest for the SN sector (0.724) and least for the ST sector (0.609). In our study, AUROC for peripapillary sectors ranged between 0.782 for IT sector to 0.71 for TL sector. The mean inside ONH CD AUROC was 0.74 and mean peripapillary RPC region CD was 0.78.

Previous studies have reported that the ONH vessel density reduction varies between 10% and 34% in glaucomatous eyes when compared to the normal eyes.<sup>6,9-11</sup> In the present study, 19% reduction was found in the mean inside disc CD and 18% reduction in the temporal sector in the POAG eyes when compared with the normal eyes. Jia et al.<sup>6</sup> (24 normal subjects and 11 glaucoma patients, Mean MD =  $-3.28$ ) reported that the reduction in ONH vessel density was greater in the temporal part of the ONH (57%), which is devoid of the major retinal vessels, when compared with the entire ONH (34%). Rao et al.<sup>9</sup> reported that the median ONH vessel density decrease was 15% inside ONH when compared with the normal eyes and the vessel density decrease in the temporal sector was 19%. Another study reported that the total ONH vessel density was reduced by 25% in glaucoma group (50 eyes) compared to the normal controls (30 eyes) and temporal vessel density was reduced by 23% in glaucoma group (mean MD =  $-10.5$ ).<sup>11</sup> This difference between the studies may be related to the definition of the ONH sectors area analyzed, definition of temporal sector, methodology used to calculate CD, suppression of large vessels during CD analysis and severity of glaucoma disease in the study population.

The inside ONH CD in our study showed a large variability when evaluated sector-wise, ranging from 11% reduction in ST sector to 30% reduction in SN sector in glaucomatous

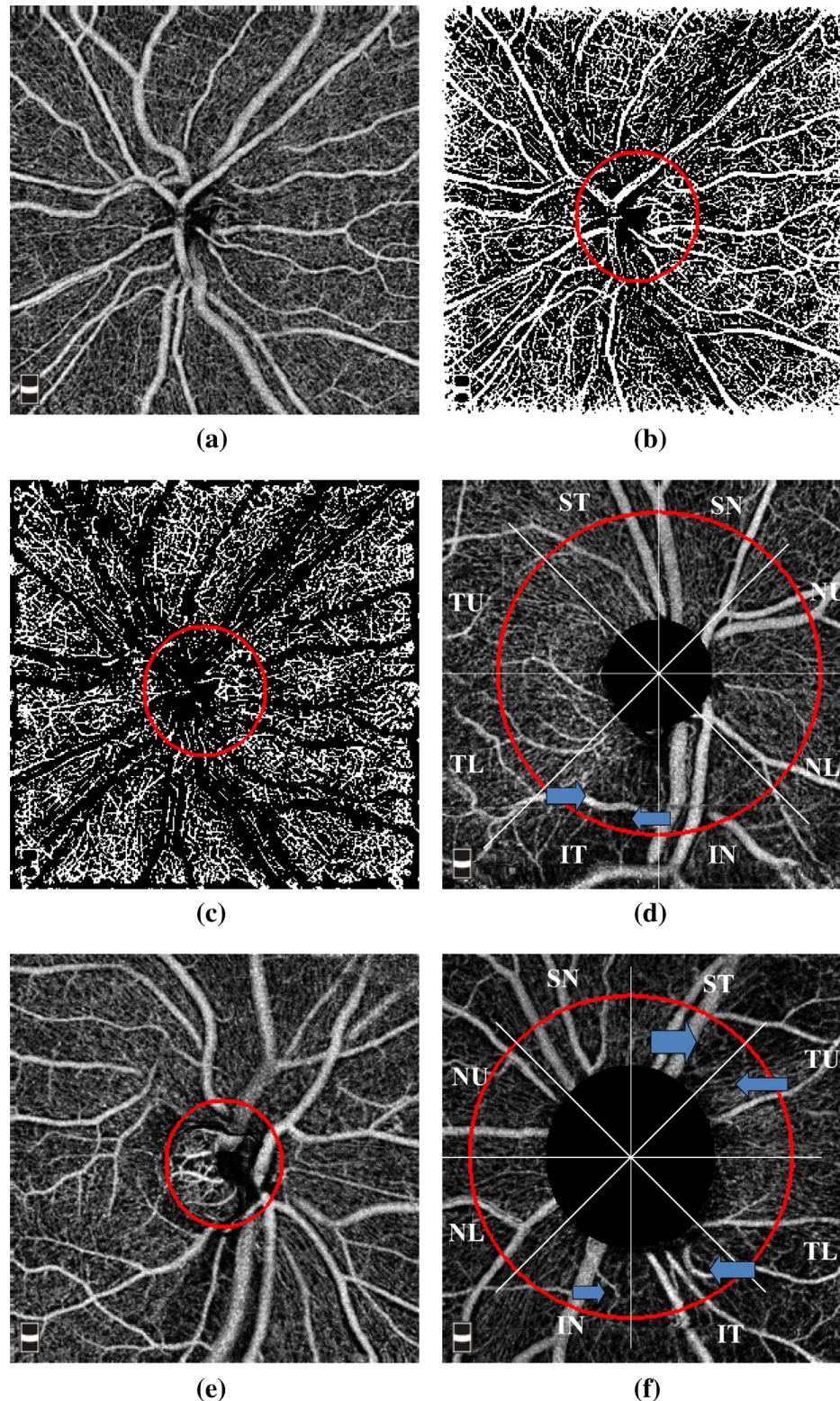


**Fig. 2.** A. Normal eyes – Dense radial peripapillary capillaries network and optic nerve head microvascular network in the enface image of optical coherence tomography angiography B. Suppression of the large vessels for the analysis. C. Capillary density image of the normal eye after suppression of the large vessels. D. Mild glaucoma – Enface optical coherence tomography angiography image shows slit shaped focal loss of radial peripapillary capillaries (arrow). E. Enface optical coherence tomography angiography of the Optic nerve head with mild attenuation of the capillaries inferiorly on the optic nerve head in a patient with mild glaucoma. F. Moderate glaucoma – Enface optical coherence tomography angiography image shows a Wedge shaped wide capillary loss in the infero-nasal and infero-temporal sectors and supero-temporal and temporal upper sector (arrow). G. Enface optical coherence tomography angiography image with attenuation of capillaries (arrow) on the Optic nerve head in an eye with moderate glaucoma. H. Severe glaucoma – Enface optical coherence tomography angiography image depicting a diffuse radial peripapillary capillary loss and in microvascular network in the Optic nerve head with diffuse loss of capillary density in the temporal sector I. Enface optical coherence tomography angiography image with diffuse loss of the capillaries on the Optic nerve head, in an eye with severe glaucoma.

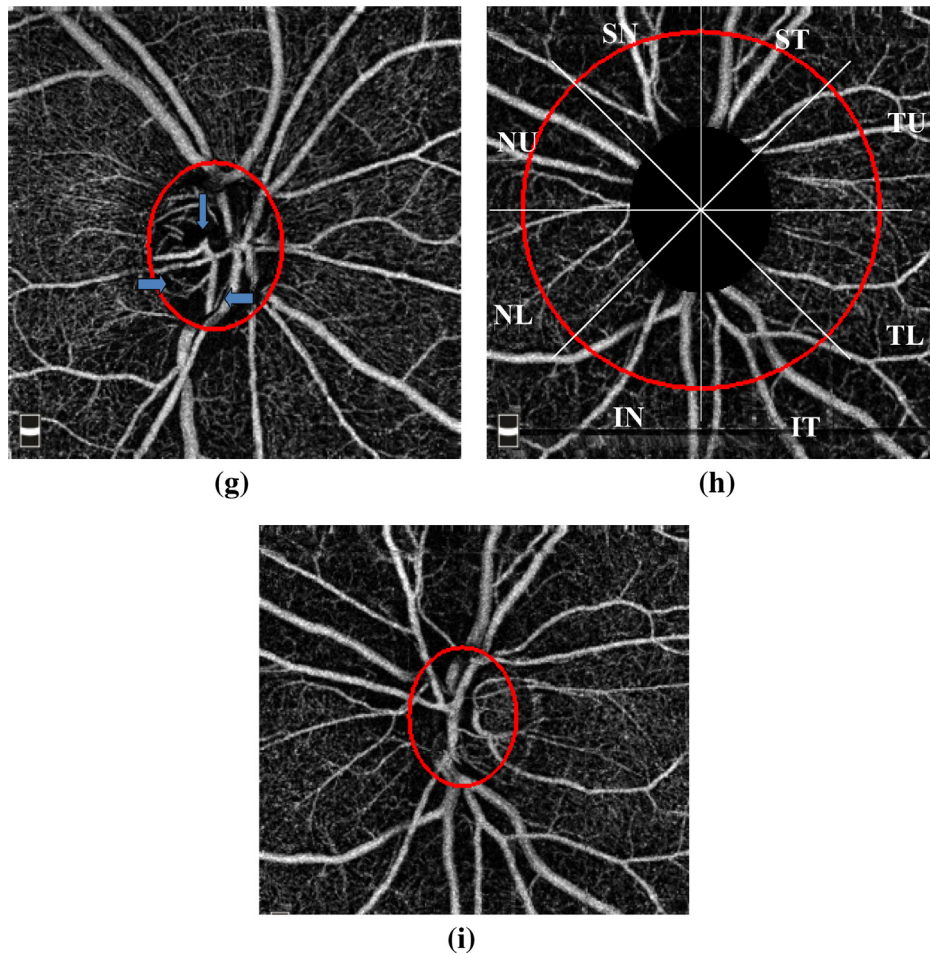


Fig. 2 (continued)

**Table 2.** Sector wise analysis of peripapillary capillary density, inside optic nerve head capillary density and retinal nerve fiber layer thickness in the glaucoma patients.

Sectorwise peripapillary CD	Glaucoma		Normal		P value
	Mean	SD	Mean	SD	
Temporal upper	0.1085	0.0417	0.1655	0.0650	<0.0001
Superior temporal	0.1562	0.0446	0.2057	0.0601	<0.0001
Superior nasal	0.0940	0.0310	0.1454	0.0555	<0.0001
Nasal upper	0.1133	0.0405	0.1687	0.0636	<0.0001
Nasal lower	0.1303	0.0456	0.1812	0.0595	<0.0001
Inferior nasal	0.0950	0.0346	0.1431	0.0604	<0.0001
Inferior temporal	0.1620	0.0499	0.2076	0.0636	<0.0001
Temporal lower	0.1103	0.0365	0.1794	0.0723	<0.0001
<i>Sectorwise inside optic nerve head CD</i>					
Temporal upper	0.1641	0.0661	0.1892	0.0507	0.04
Superior temporal	0.1352	0.0557	0.1527	0.0455	<b>0.095</b>
Superior nasal	0.0973	0.0475	0.1399	0.0515	<0.0001
Nasal upper	0.1232	0.0519	0.1494	0.0457	0.01
Nasal lower	0.1336	0.0548	0.1570	0.0534	0.04
Inferior nasal	0.1083	0.0494	0.1256	0.0445	<0.0001
Inferior temporal	0.1338	0.0511	0.1543	0.0478	0.045
Temporal lower	0.1655	0.0606	0.2127	0.0503	<0.0001

CD: Capillary density.  
SD: Standard deviation.

**Table 3.** Area under receiver operator curve (AUROC) for the inside optic nerve head (ONH) capillary density (CD) and peripapillary CD to differentiate between the normal and glaucomatous eye using optical coherence tomography angiography.

Variables	AUROC	Standard error	95% confidence interval Lower bound	95% confidence interval Upper bound	P value
<i>Sector-wise optic nerve head capillary density (CD)</i>					
Superior temporal	<b>0.609</b>	0.058	0.495	0.723	<b>0.065</b>
Temporal upper	0.617	0.058	0.504	0.730	<b>0.048</b>
Superior nasal	<b>0.724</b>	0.051	0.624	0.825	<0.0001
Nasal upper	0.663	0.055	0.555	0.771	0.006
Temporal lower	0.713	0.053	0.609	0.816	<0.0001
Inferior temporal	0.638	0.057	0.526	0.749	0.020
Nasal lower	0.673	0.055	0.564	0.781	0.004
Inferior nasal	0.633	0.058	0.519	0.748	0.024
<b>Mean ONH CD</b>	<b>0.743</b>	0.052	0.642	0.844	<0.0001
<i>Sector-wise peripapillary capillary density (CD)</i>					
Temporal upper	0.747	0.040	0.668	0.826	<0.0001
Superior temporal	0.761	0.040	0.682	0.840	<0.0001
Superior nasal	0.774	0.038	0.699	0.850	<0.0001
Nasal upper	0.760	0.039	0.683	0.837	<0.0001
Nasal lower	0.751	0.039	0.675	0.827	<0.0001
Inferior nasal	0.745	0.040	0.666	0.824	<0.0001
Inferior temporal	<b>0.782</b>	0.038	0.708	0.857	<0.0001
Temporal lower	<b>0.710</b>	0.042	0.626	0.793	<0.0001
<b>Mean peripapillary CD</b>	<b>0.784</b>	0.038	0.709	0.859	<0.0001

eyes when compared with the normal subjects. The variability was less when analyzed quadrant-wise, i.e., 13% CD reduction for the inferior quadrant to 20% CD reduction for superior quadrant in the glaucomatous eyes.

Previous OCT-A studies have reported 11–13% reduction of peripapillary vessel density in glaucoma patients when compared to normal controls.<sup>8,9</sup> Liu et al.<sup>8</sup> assessed both the superficial and deep capillary beds and calculated the vascular parameters in a thicker retinal slab from the ILM to the RPE. We found 29% reduction in the mean RPC peripapillary CD in glaucomatous eyes when compared to the normal eyes. This difference among the studies could be because of the fact that the severity of glaucoma in our study patients (Mean MD: -12.D) was more than that in the other reported studies.<sup>8,9</sup> Also, we used B-COSFIRE method for the automatic segmentation of blood vessels and suppressed the large vessels during CD analysis and the methodology used to calculate ONH CD and RPC was different.

The difference in the two scanning region for the CD measurement i.e. peripapillary RPC and ONH region could be due to the physiological variations in the disc size and shape, disc tilt, area of peripapillary atrophy (PPA), position of exit of the major trunk of central retinal vessels on the ONH surface. However, we did not find a significant correlation between the disc size and ONH CD measurements in normal and POAG eyes. Also, we did not measure the area of PPA in our study, though none of the patients had significant PPA.

The limitations of the current study is that we did not evaluate the possible confounding effect of Diabetes mellitus, systemic hypertension, ocular perfusion pressure, ocular anti-hypertensive medications and AGM on the CD measurement. Therefore, we could not rule out the impact of systemic diseases, medications and AGM on the CD measurements.

## Conclusion

The present study demonstrated that OCT-A derived RPC density and inside ONH CD is significantly reduced in the

POAG eyes when compared with the healthy control eyes. These parameters have a moderate diagnostic accuracy for discriminating healthy eyes from glaucoma patients. Diagnostic ability of even the best parameter, i.e., mean and IT sector peripapillary sector RPC CD and SN sector and mean ONH CD parameter was only moderate. Further studies are needed to determine the usefulness of the peripapillary RPC CD and ONH CD loss, found in the POAG patients in the glaucoma diagnosis.

## Conflict of interest

The authors declared that there is no conflict of interest.

## Financial interest

None.

## References

- Bonomi L, Marchini G, Marraffa M, et al. Vascular risk factors for primary open angle glaucoma: the Egna-Neumarkt Study. *Ophthalmology* 2000;**107**:1287–93.
- Henkind P. Radial peripapillary capillaries of the retina. I. Anatomy: human and comparative. *Br J Ophthalmol* 1967;**51**:115–23.
- Alterman M, Henkind P. Radial peripapillary capillaries of the retina. II. Possible role in Bjerrum scotoma. *Br J Ophthalmol* 1968;**52**:26–31.
- Kornzweig AL, Eliasoph I, Feldstein M. Selective atrophy of the radial peripapillary capillaries in chronic glaucoma. *Arch Ophthalmol* 1968;**80**:696–702.
- Yarmohammadi A, Zangwill LM, Diniz-Filho A, et al. Optical coherence tomography angiography vessel density in healthy, glaucoma suspect and glaucoma eyes. *Invest Ophthalmol Vis Sci* 2016;**57**:451–9.
- Jia Y, Wei E, Wang X, et al. Optical coherence tomography angiography of optic disc perfusion in glaucoma. *Ophthalmology* 2014;**121**:1322–32.
- Mammo Z, Heisler M, Balaratnasingam C, et al. Quantitative optical coherence tomography angiography of radial peripapillary capillaries in glaucoma, glaucoma suspect, and normal eyes. *Am J Ophthalmol* 2016;**170**:41–9.

- 392 8. Liu L, Jia Y, Takusagawa HL, et al. Optical coherence tomography  
393 angiography of the peripapillary retina in glaucoma. *JAMA*  
394 *Ophthalmol* 2015;**133**:1045–52.
- 395 9. Rao HL, Pradhan ZS, Weinreb RN. etc. Regional comparisons of  
396 optical coherence tomography angiography vessel density in primary  
397 open angle glaucoma. *Am J Ophthalmol* 2016;**171**:75–83.
- 398 10. Wang X, Jiang C, Ko T, et al. Correlation between optic disc  
399 perfusion and glaucomatous severity in patients with open-angle  
400 glaucoma: an optical coherence tomography angiography study.  
401 *Graefes Arch Clin Exp Ophthalmol* 2015;**253**:1557–64.
- 402 11. Lévêque PM, Zéboulon P, Brasnu E, et al. Optic disc vascularization in  
403 glaucoma: value of spectral-domain optical coherence tomography  
404 angiography. *J Ophthalmol* 2016. [https://doi.org/10.1155/2016/](https://doi.org/10.1155/2016/6956717)  
405 [6956717](https://doi.org/10.1155/2016/6956717), Epub Feb 22. 2016:6956717.
- 406 12. Jia Y, Tan O, Tokayer J, et al. Split-spectrum amplitude decorrelation  
407 angiography with optical coherence tomography. *Opt Express*  
408 2012;**20**:4710–25.
- 409 13. Azzopardi George, Strisciuglio Nicola, Vento Mario, et al. Trainable  
410 cosfire filters for vessel delineation with application to retinal images.  
411 *Med Image Anal* 2015;**19**:46–57.
- 412 14. Mansoori T, Sivaswamy J, Gamalapati JS, et al. Measurement of  
413 radial peripapillary capillary density in the normal human retina using  
414 optical coherence tomography angiography. *J Glaucoma*  
415 2017;**26**:241–6.
- 416 15. Kraus MF, Potsaid B, Mayer MA, et al. Motion correction in optical  
417 coherence tomography volumes on a per A-scan basis using  
418 orthogonal scan patterns. *Biomed Opt Express* 2012;**3**:1182–99.
- 419 16. Anderson DR, Patella VM. *Automated static perimetry*. 2nd ed. St.  
420 Louis: Mosby; 1999. p. 121–36.
- 421